

Electronic Supplementary Information

Kinetic Modeling of Multi-Step Transformations Using Sequential Dynamic Flow Experiments

Klara Silber,^{a,b} Florian L. Wagner,^{a,b} Christopher A. Hone,^{*a,b} and C. Oliver
Kappe^{*a,b}

^aCenter for Continuous Flow Synthesis and Processing (CC FLOW), Research Center
Pharmaceutical Engineering GmbH (RCPE), Inffeldgasse 13, Graz, Austria

^bInstitute of Chemistry, University of Graz, Heinrichstrasse 28, 8010 Graz, Austria.

Email: christopher.hone@rcpe.at, oliver.kappe@uni-graz.at

Table of Contents

1	General Information.....	2
1.1	Materials and Flow Equipment	2
2	General Flow Configuration.....	2
2.1	Paal Knorr reaction	2
2.2	Telescoped reaction.....	3
3	Automation.....	5
4	Process Analytical Technology (PAT)	5
4.1	Inline FTIR.....	5
4.1.1	PLS Model	5
4.2	Online UHPLC.....	7
4.2.1	Calibration	8
5	Residence Time Distribution	9
6	Dynamic experiments Paal Knorr reaction.....	11
6.1	Validation Dynamic Experimentation with Steady State Experiment	12
6.2	Comparison FTIR with UHPLC	13
7	Kinetic fitting of the Paal Knorr reaction in Dynochem.....	13
7.1	Model validation	16
8	Dynamic experiments telescoped reaction	17
8.1	Validation Experiments.....	18
8.2	Mass balance	18
9	Kinetic fitting of the nucleophilic aromatic substitution in Dynochem.....	19
9.1	Validation of the kinetic model.....	21
10	References.....	21

1 General Information

1.1 Materials and Flow Equipment

Solvents and chemicals were obtained from commercial suppliers and were used without any further purification. The percentages shown in brackets following the chemicals indicate the reported purity from the supplier. Ethylenediamine (**1**, 99%), 2-fluoronitrobenzene (**5**), 1,1,3,3-tetramethylguanidine (**6**, TMG, 99%) and acetonitrile (HPLC Plus, $\geq 99.9\%$) were purchased from Sigma Aldrich. 2,5-hexandione (**2**, 97%) was purchased from Thermo Scientific. 2-*tert*-butyl-1,1,3,3-tetramethylguanidine was purchased from TCI ($> 95\%$). In the flow setup, standard PFA tubing (0.3 mm, 0.8 mm or 1.6 mm i.d.), fittings, T-pieces manufactured from PTFE or PEEK were used as connectors.

2 General Flow Configuration

2.1 Paal-Knorr Pyrrole Reaction

Stock solutions were prepared with the following procedure.

1.1 M 2,5-hexandione (**1**) stock solution: A 250 mL volumetric flask was charged with 31.38 g of **1** and filled up to the 250 mL mark with acetonitrile.

0.9 M ethylenediamine (**2**) stock solution: A 250 mL volumetric flask was charged with 13.52 g of **2** and 6.84 g of dibenzyl and filled up to the 250 mL mark with acetonitrile.

The reaction was performed in a 4.23 mL coil reactor (PFA tubing, 0.8 mm i.d.) and the reaction stream was analyzed using a Mettler Toledo ReactIR 702L and a Shimadzu Nexera X2 UHPLC (**Figure S1**).

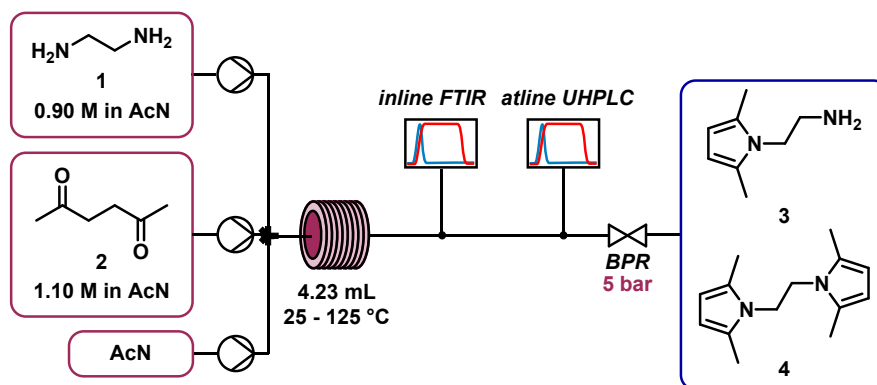


Figure S1. Reaction and PAT setup to study the Paal Knorr reaction.

The feed solutions were delivered using Knauer AZURA P 4.1S HPLC pumps (10 mL/min pump head, Hastelloy/ceramic with pressure sensor). A back pressure regulator (BPR, Upchurch, P-465) equipped with a 34 bar (green, P-765) cartridge was attached directly after each HPLC pump. A 7-port mixer was used to combine the inlet streams. The coil reactor (4.23 mL, PFA tubing, 0.8 mm i.d.) was connected using a PFA tubing (0.15 mL, 0.8 mm i.d.) and heated using a thermostat (Huber, Ministat 240). It was further connected with a PFA tubing (0.35 mL, 0.08 mm i.d.) to an inline FTIR (Mettler Toledo, React

IR 702L) with a flow cell (Mettler Toledo, DS Micro Flow Cell Diamond) where the reaction mixture was analyzed. A PTFE tubing (0.10 mL, 0.3 mm i.d.) was used to connect the outlet of the FTIR to the sampling point of the UHPLC (Shimadzu, Nexera X2). A membrane-based BPR (Zaiput, BPR-10), set to 5 bar was integrated after the UHPLC.

2.2 Telescoped Reaction

Stock solutions were prepared according to the following procedure.

0.96 M 2,5-hexandione (1) stock solution: A 100 mL volumetric flask was charged with 10.96 g of **1** and filled to the 100 mL mark with acetonitrile.

0.8 M ethylenediamine (2) stock solution: A 100 mL volumetric flask was charged with 4.81 g of **2** and 1.82 g of dibenzyl and filled to the 100 mL mark with acetonitrile.

0.4 M 2-fluoronitrobenzene (3) + 0.6 M 1,1,3,3-tetramethylguanidine (4) stock solution: A 100 mL volumetric flask was charged with 5.64 g of **3**, 6.91 g of **4** and 2.02 g of 1,3,5-trimethoxybenzene and filled to the 100 mL mark with acetonitrile.

The first reaction step (Paal-Knorr pyrrol reaction) was performed in a 12.0 mL coil reactor (PFA tubing, 1.6 mm i.d.) and operated at steady state conditions to ensure full conversion of ethylenediamine. A reservoir was used in-between reaction steps to allow variation of the input concentration in the second reaction (S_NAr) reaction (**Figure S2** and **Figure S3**).

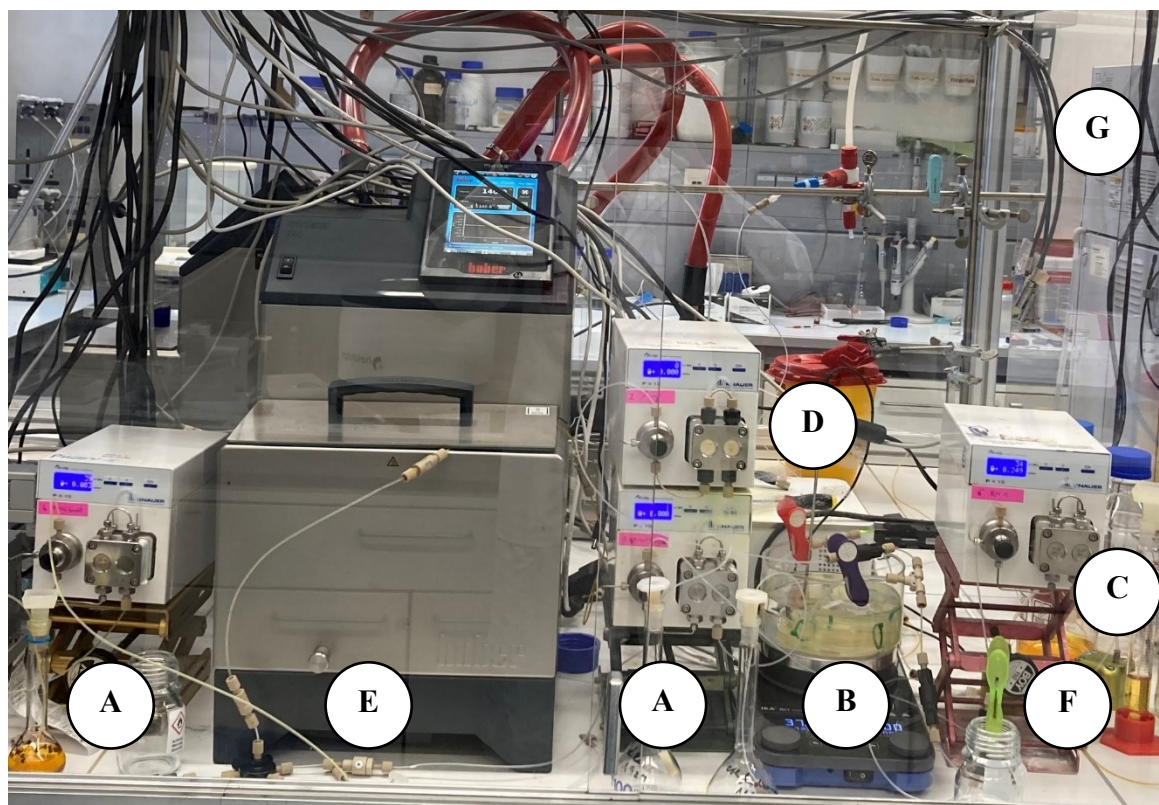


Figure S2. Photograph of the reaction setup in the lab for the telescoped reaction, showing the following equipment: A: HPLC Pumps, B: Reactor Paal-Knorr reaction, C: Reservoir, D: React IR 702L, E: Thermostat with reactor for S_NAr reaction, F: BPR, G: UHPLC.

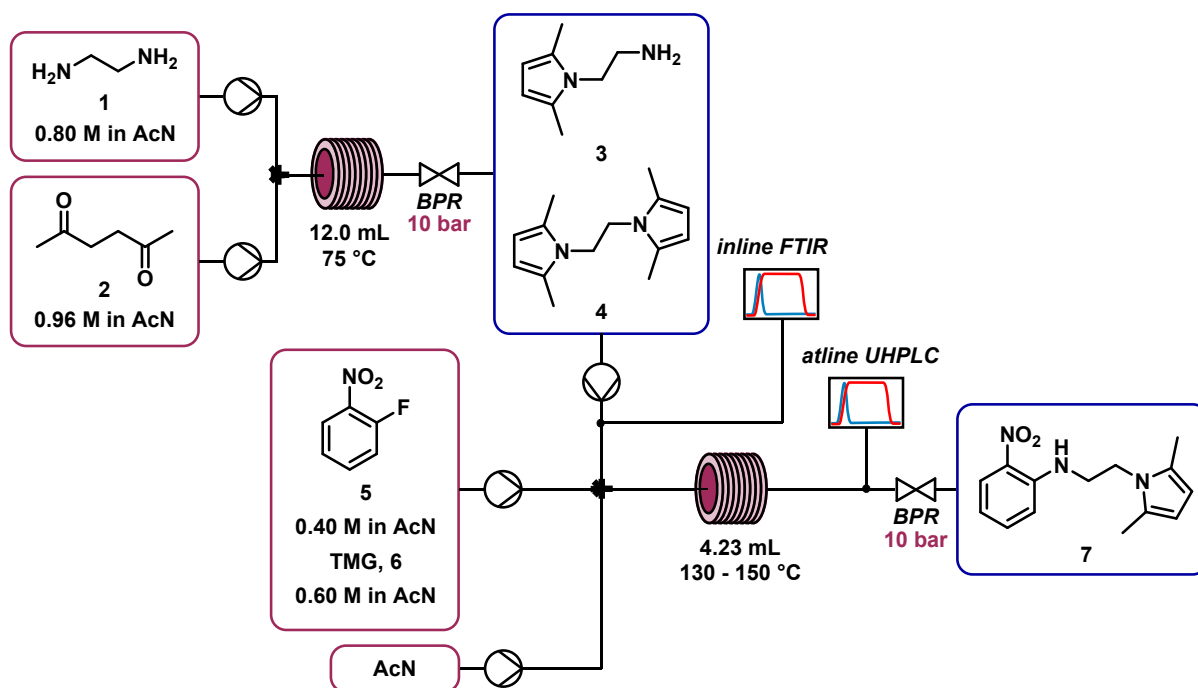


Figure S3. Reaction and PAT setup to study the S_NAr reaction as telescoped reaction.

The feed solutions were pumped with Knauer AZURA P 4.1S HPLC pumps (10 mL/min pump head, made of Hastelloy C/stainless steel/ceramic with an integrated pressure sensor). A back pressure regulator (BPRs, Upchurch cartridge holder, P-465) equipped with a 34 bar (tan/green, P-765) cartridge was attached directly after each HPLC pump. Ethylenediamine **1** and 2,5-hexanedione **2** stock solutions were combined with a T-piece mixer and pumped to the heated coil reactor (PFE tubing, 12.0 mL, 1.6 mm i.d.) using a connection tube (0.15 mL, 0.8 mm i.d., PFA tubing). The coil was connected *via* a PFA tubing (0.20 mL, 0.8 mm i.d.) to a membrane-based BPR (Zaiput, BPR-10) set to 10 bar and collected in a reservoir (100 mL). The reaction mixture from the Paal Knorr reaction was directly used as the feed solution for the S_NAr reaction and analyzed using the inline FTIR (Mettler Toledo, React IR 702L, DS Micro Flow Cell Diamond) directly before combining the reaction stream with the streams of the 2-fluoronitrobenzene **5** and TMG **6** stock solution and acetonitrile *via* a 7-port mixer. A check valve was included directly before the mixer in the Paal-Knorr reaction stream. PFA tubings were used as connections (0.15 mL, 0.8 mm i.d., PFA tubing, from the mixer to the reactor, 0.20 mL, 0.3 mm i.d., PTFE tubing, from the reactor to the UHPLC). The coil reactor (4.23 mL, PFA tubing, 0.8 mm i.d.) was heated using a thermostat (Huber, Ministat 240). The reaction mixture was analyzed using online UHPLC (Shimadzu, Nexera X2). A membrane-based BPR (Zaiput, BPR-10), set to 10 bar was integrated into the reaction setup after the UHPLC.

3 Automation

The HPLC pumps and the thermostat were connected *via* RS232 to the HiTec Zang LabManager. The ramps for the flow rates and temperature were programmed in HiText (HiTec Zang) and the setpoints for the HPLC pumps and the thermostat were set in LabVision software (HiTec Zang).

4 Process Analytical Technology (PAT)

4.1 Inline FTIR

Inline FTIR spectra were recorded on a Mettler Toledo ReactIR 702L equipped with a flow cell (Mettler Toledo, DS Micro Flow Cell Diamond). The acquisition time for each data point was 15 s. Spectra were recorded between 4000 and 600 cm^{-1} using the maximum resolution of 4 cm^{-1} . The obtained spectra were exported by the iCIR7 software and automatically read and processed with a PLS model using Peaxact Process Link (S-PACT).

4.1.1 PLS Model

The training samples were obtained from calibration solutions from mixtures of 2,5-hexandione (**2**), ethylenediamine (**1**), product (**3**), overreacted product (**4**) and dibenzyl as internal standard. Product (**3**) and overreacted product (**4**) were synthesized from **1** and **2** stoichiometric amounts in *iso*-propanol. Product (**3**) was further purified by column chromatography. In total, 21 calibration solutions from pure compounds and mixtures of the compounds were prepared in 5 mL volumetric flasks in concentration ranges from 50-400 mmol/L. Each sample was injected to the IR flow cell and at least five spectra were collected for each sample. The acquired training spectra were read into PEAXACT 5.3 (S-PACT) and processed with the following pretreatment conditions. The global range was set to 800-3500 cm^{-1} , where the diamond region was excluded from 1888-2500 cm^{-1} . A rubber band subtraction was used for baseline correction and the spectra were further processed using 2nd derivative with a filter length of 5. A sample spectrum of the reaction mixture before and after pre-processing is shown in **Figure S4** and **Figure S5**. The following ranks were set for the components in the PLS model with the resulting root-mean-square error of calibration (RMSE_C) and root-mean-square error of cross validation (RMSE_{CV}) performance indicators: 2,5-hexandione (**2**) (rank 1, R^2 : 0.997, RMSE_C : 4.2 mM, RMSE_{CV} : 4.3 mM), product (**3**) (rank 3, R^2 : 0.991, RMSE_C : 8.5 mM, RMSE_{CV} : 8.8 mM), overreacted product (**4**) (rank 3, R^2 : 0.974, RMSE_C : 12 mM, RMSE_{CV} : 13 mM). Cross-validation was performed using K-fold partitioning using a K value of 10 resulting in the -mean-square error of cross-validation (RMSE_{CV}). The predicted vs. true plots for the PLS models are shown in **Figure S6**.

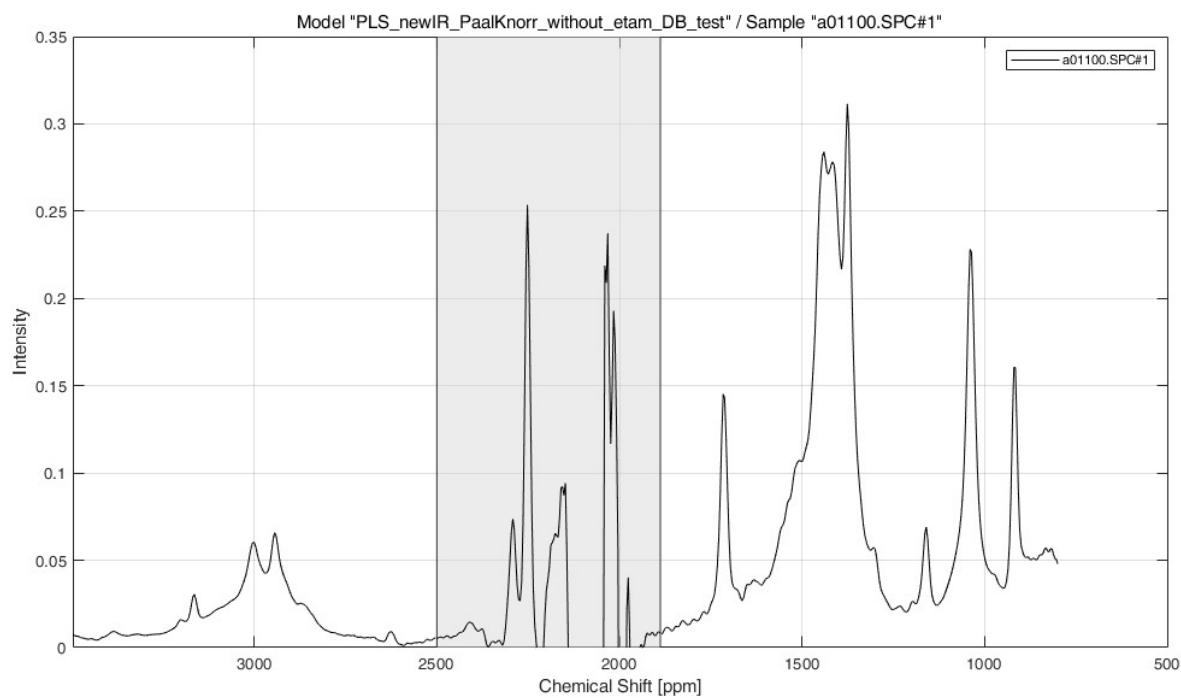


Figure S4. FTIR spectrum of the Paal Knorr reaction mixture before pretreatment.

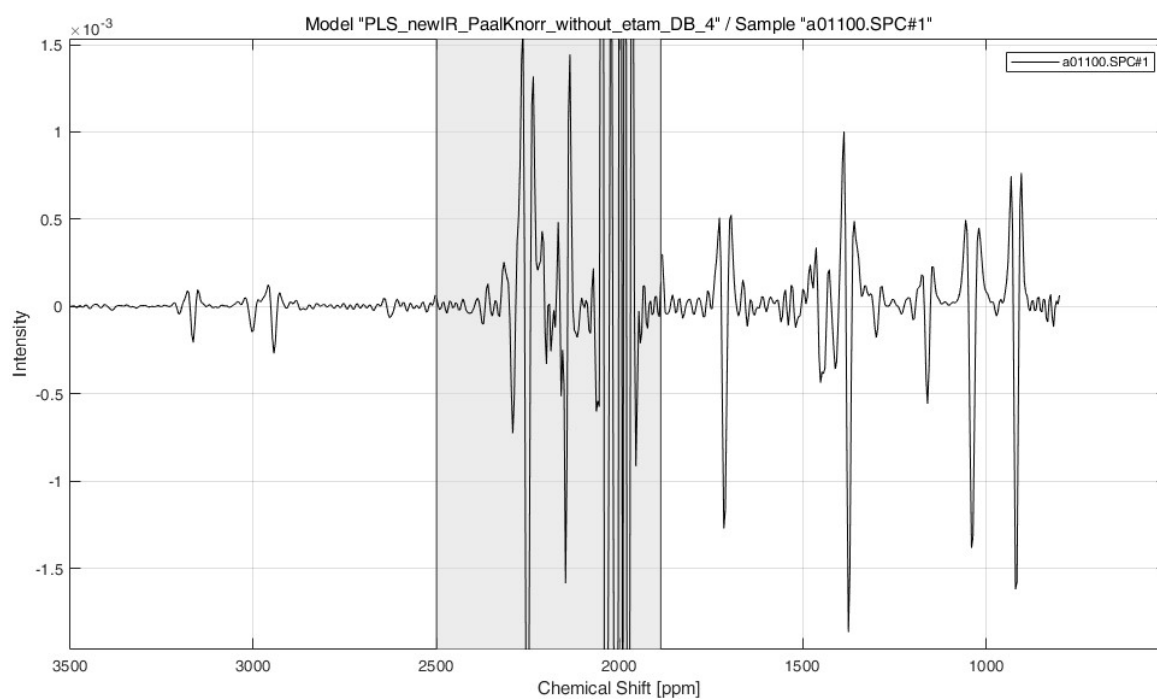


Figure S5. FTIR spectrum of the Paal Knorr reaction mixture after pretreatment by using the second derivative and a smoothing filter.

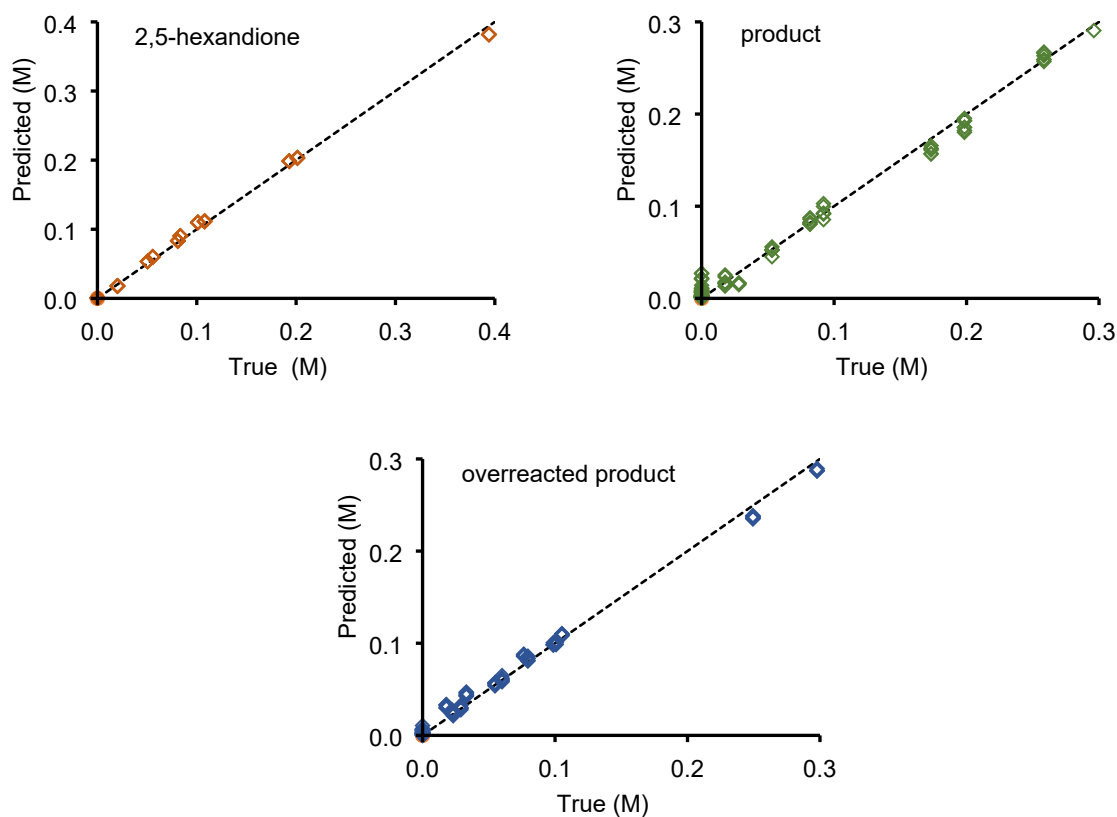


Figure S6. Predicted vs. true plots of 2,5-hexandione (**2**) (top), product (**3**) (top) and overreacted product (**4**) (bottom).

4.2 Online UHPLC

The UHPLC-DAD (Shimadzu, Nexera X2) consists of a degassing unit (DGU-403ASR), two solvent delivery units (LC-30AD), a thermostated column oven (CTO-20AC), a diode array detector (SPD-M30A) and a control unit (CBM-20A). Analysis was carried out using a reversed-phase column (Phenomenex Luna Omega C18 (50 x 2.1 mm, particle size 1.6 μm , pore size 100 \AA)) at 45 $^{\circ}\text{C}$ using a total flow rate of 1 mL/min. The sample was introduced by an internal injection valve (10 nL, 20000 psi, Cheminert Nanovolume, Part# C84U-6674-.01EUH), which was triggered by the CBM-20A controller.

Solvent A: $\text{H}_2\text{O} + \text{MeCN } 9 + 1 \text{ (v/v)} + 0.1\% \text{ HCOOH}$

Solvent B: $\text{MeCN} + 0.1\% \text{ HCOOH}$

Method:

- 0.00-0.50 min: 5% solvent B
- 0.50-1.20 min: ramp to 60% solvent B
- 1.20-1.75 min: ramp to 65% solvent B
- 1.75-2.20 min: ramp to 90% solvent B
- 2.20-2.50 min: ramp to 100% solvent B
- 2.51 min: 5% solvent B

A sample chromatogram of the reaction mixture at 215 nm is shown in **Figure S7**.

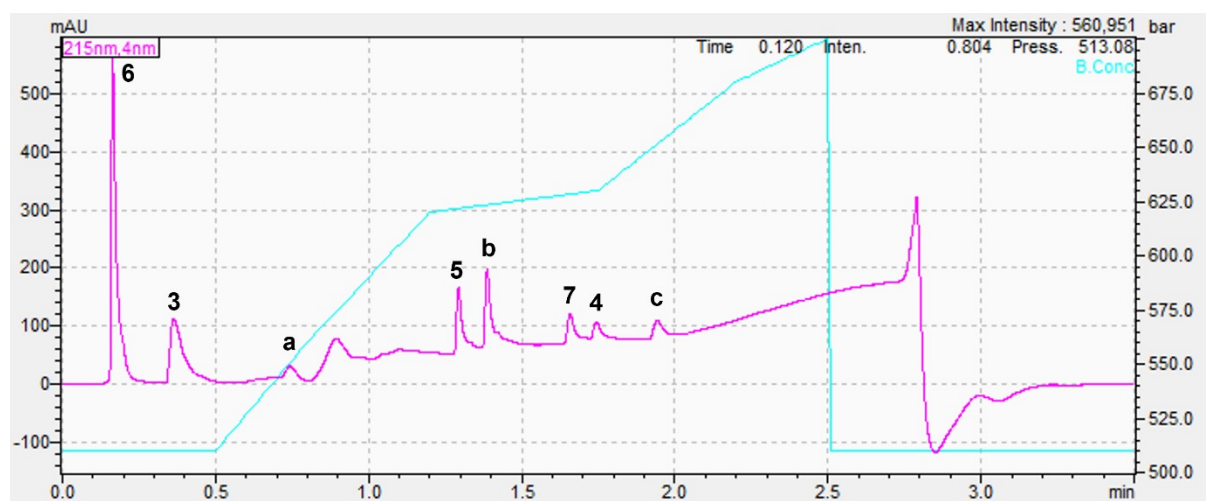


Figure S7. Typical chromatogram of the reaction mixture at 215 nm. Peaks can be assigned to: TMG (**6**), product (**3**), impurity (**a**), 2-fluoronitrobenzene (**5**), 1,3,5-trimethoxybenzene (**b**), S_NAr product (**7**), overreacted product (**4**), dibenzyl (**c**). The peak at 0.9 min is an artefact of the method and is also present in blank samples of pure acetonitrile. The gradient is shown in cyan.

4.2.1 Calibration

Calibration solutions of product (**3**) and overreacted product (**4**) with 30 mmol/L dibenzyl and calibration solutions of 2-fluoronitrobenzene (**5**) and S_NAr product (**7**) with 30 mmol/L 1,3,5-trimethoxybenzene were prepared in 5 mL volumetric flasks in acetonitrile. S_NAr product (**7**) was synthesized from **5** and **3** in equimolar amounts at room temperature in DMSO using 1.5 equiv. 1,8-Diazabicyclo[5.4.0]undec-7-ene (DBU) as base. Purification was done by column chromatography. Each calibration solution was analyzed three times. All compounds were calibrated based on peak areas at 215 nm (**Figure S8**).

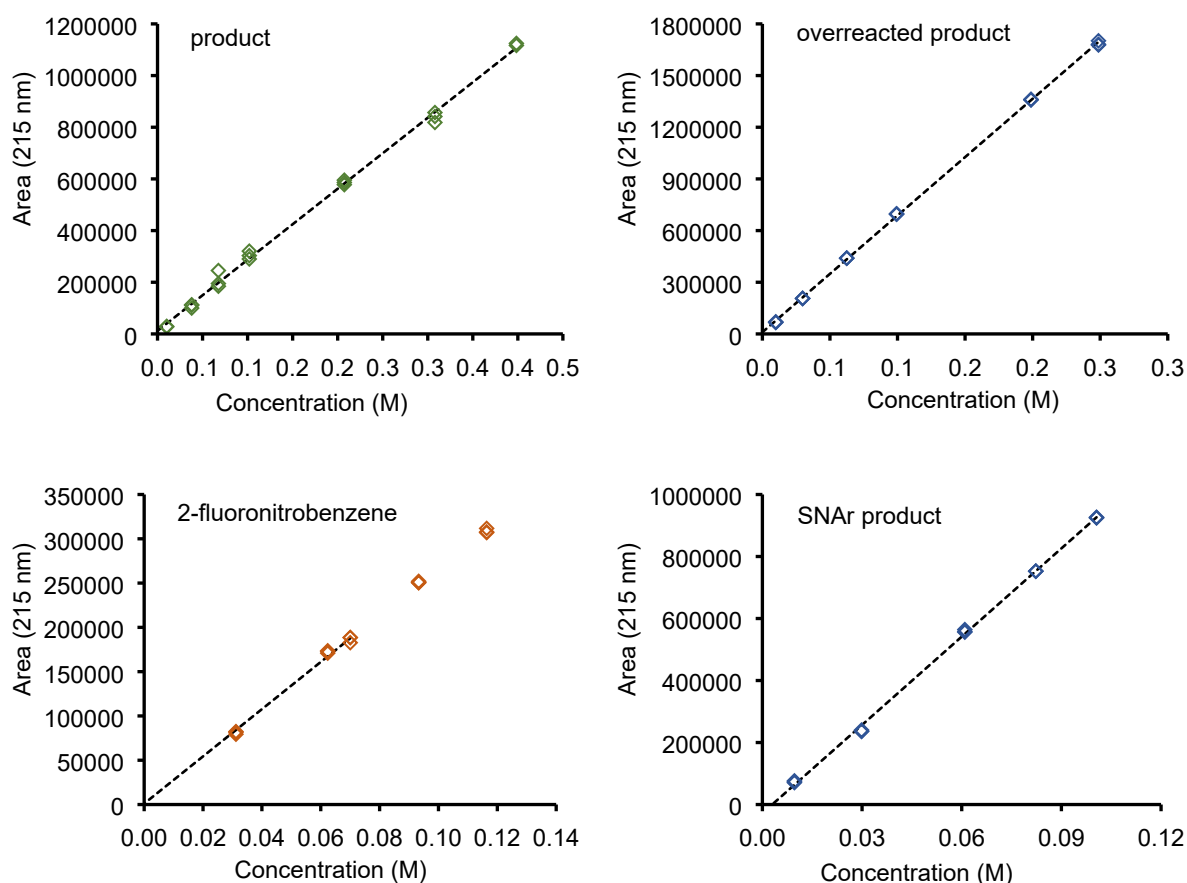


Figure S8. Calibration curve for online UHPLC analysis of product (3) (top left), overreacted product (4) (top right), 2-fluoronitrobenzene (5) (bottom left) and S_NAr product (7) (bottom right) at a wavelength of 215 nm.

5 Residence Time Distribution (RTD)

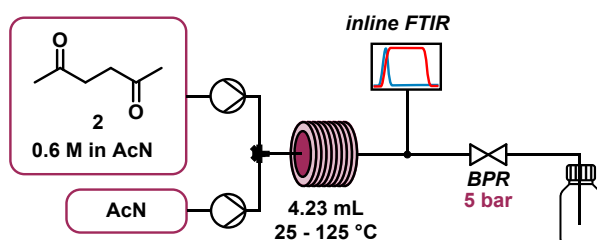


Figure S9. Reaction and PAT setup to study residence time distribution.

The flow setup (**Figure S9**) was used to automatically determine the residence time distribution at five different temperatures (25 °C, 50 °C, 75 °C, 100 °C and 125 °C) and three different flow rates (2 mL/min, 1 mL/min, 0.5 mL/min). The residence times were investigated by changing the concentration of 2,5-hexandione using a step up (0 mol/L to 0.3 mol/L) followed by a step down (0.3 mol/L to 0 mol/L) function. Concentration values after the reactor were obtained using inline FTIR.

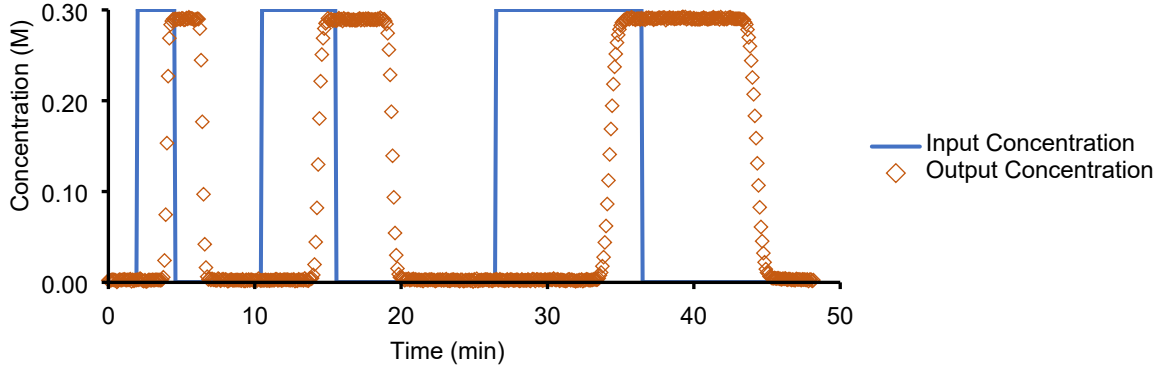


Figure S10. Experimental design of experiments for RTD investigations with input concentrations and output concentrations measured by inline FTIR. Data shown from experiments at 75 °C. Output concentrations were corrected by the minimal offset from the dataset.

Residence time, Bodenstein number and axial dispersion number were calculated as described in Levenspiel^[1] and given for the experiments at 75 °C (**Figure S10**) in **Table S1**. The mean residence time t_{res} was calculated according to **Equation 1**, where t_i is the time from the start of the step input, Δc_i the concentration difference between two adjacent measurement points and c_{max} the maximum concentration within an experiment.

$$t_{res} \cong \frac{\sum_i t_i \cdot \Delta c_i}{c_{max}} \text{ with } \Delta c_i = c_i - c_{i-1} \quad (1)$$

The variance σ^2 (**Equation 2**) represents the spread of the distribution when it passes the reactor outlet.

$$\sigma^2 \cong \frac{\sum_i t_i^2 \cdot \Delta c_i}{c_{max}} - t_{res}^2 \quad (2)$$

The variance was used to obtain the Bodenstein number Bo (**Equation 3**). A Bodenstein number higher than 100 indicates plug flow behavior, while a value below 100 indicates more CSTR-like behavior.

$$Bo = \frac{2 \cdot t_{res}^2}{\sigma^2} \quad (3)$$

The axial dispersion number D_{ax} was calculated according to **Equation 4** where u is the flow velocity and L the length of the reactor.

$$D_{ax} = \frac{u \cdot L}{Bo} \quad (4)$$

Table S1: Calculated residence time, Bodenstein number and axial dispersion number at a reactor temperature of 75 °C.

Flow rate (mL/min)	t_{res} (s)	Bo (-)	D_{ax} (m ² /s)
2.00	122	603	9.2E-4
1.00	235	770	3.6E-4
0.50	469	1008	1.4E-4

The Bodenstein number is higher than 100, therefore plug flow behavior can be assumed and the impact of axial dispersion is negligible.

The average residence time at a certain flow rate is temperature dependent and can be assumed to be directly proportional to the density of the solvent.

6 Dynamic Experiments Paal-Knorr Pyrrole Reaction

The process setup is described in **Section 2 (Figure S1)**. All dynamic experiments were performed at constant temperature and constant concentration of ethylenediamine (**1**) and 2,5-hexandione (**2**) while linearly varying the flow rate. An initial equilibration of the system with steady state conditions was held for 7 min followed by a ramp of the flow rate from 2 mL/min to 0.25 mL/min for 60 min followed by a constant flow rate of 0.25 mL/min for 25 min (**Figure S11**). The residence time during the ramps was calculated according to **Equation 5** where v_0 is the initial flow rate in mL/min, α_v is the slope for the change of the flow rate in mL/min², V is the total volume in mL for the calculation of $t_{in,i}$ the inlet time or the volume from the reactor to the analytics for the calculation on $t_{L,i}$, and $t_{m,i}$ is time passed from starting the flow rate in min.^[2] The residence can then be calculated as the difference between $t_{L,i}$ and $t_{in,i}$.

$$t_{L,i \text{ or } In,i} = \frac{v_0 - \sqrt{v_0^2 - 2\alpha_v \cdot (v_0 \cdot t_{m,i} - 0.5\alpha_v t_{m,i}^2 - V)}}{\alpha_v} \quad (5)$$

Table S2: Conditions of dynamic experiments for the kinetic study of the Paal-Knorr pyrrole reaction.

Exp	Conc. ethylenediamine (mol/L)	Equiv. 2,5-hexandione	T (°C)
1	0.3	1.0	50
2	0.4	1.2	50
3	0.2	1.4	50
4	0.3	1.6	50
5	0.4	1.0	75
6	0.2	1.2	75
7	0.4	1.4	75
8	0.3	1.6	75
9	0.3	1.0	100
10	0.2	1.2	100
11	0.3	1.4	100
12	0.2	1.6	100
13	0.3	1.4	25
14	0.3	1.4	125

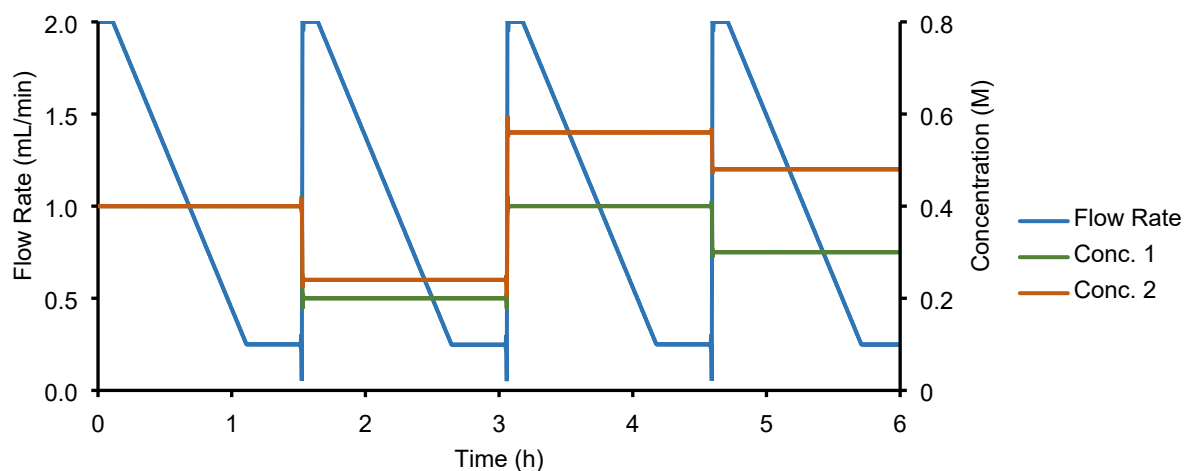


Figure S11: Experimental conditions for experiments 5-8 at 75 °C. Linear variation of flow rate while concentration of ethylenediamine (1) and 2,5-hexandione (2) remains constant for each experiment.

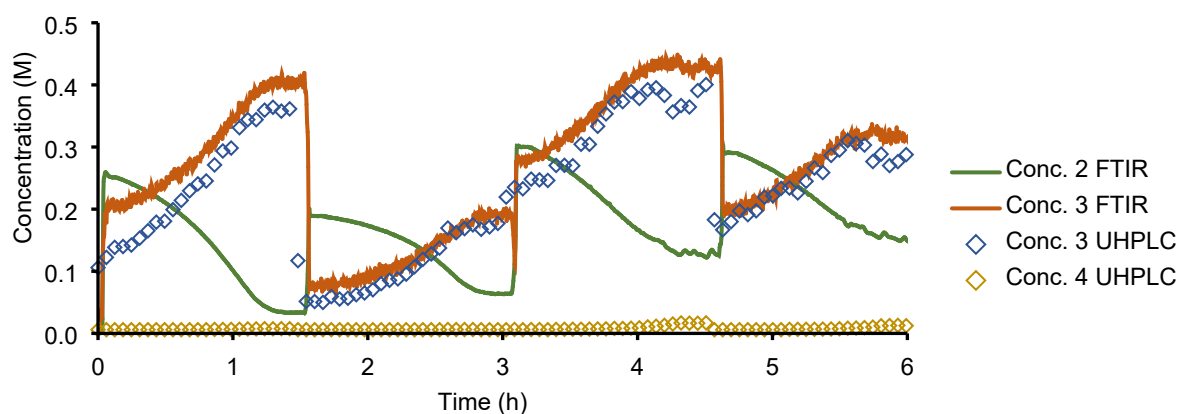


Figure S12: Experimental data for experiments 5-8 (Table S2) at a temperature of 75 °C. Measured FTIR concentrations of 2,5-hexandione (2) and product (3) and UHPLC concentrations of product (3) and overreacted product (4) are shown in the diagram. Almost no overreacted product (4) was formed.

6.1 Validation Dynamic Experimentation with Steady State Experiment

To verify the validity of the dynamic experimentation approach, reactions at steady state conditions at 75°C and flow rates of 2 mL/min, 1 mL/min, 0.5 mL/min and 0.33 mL/min were performed (Figure S13).

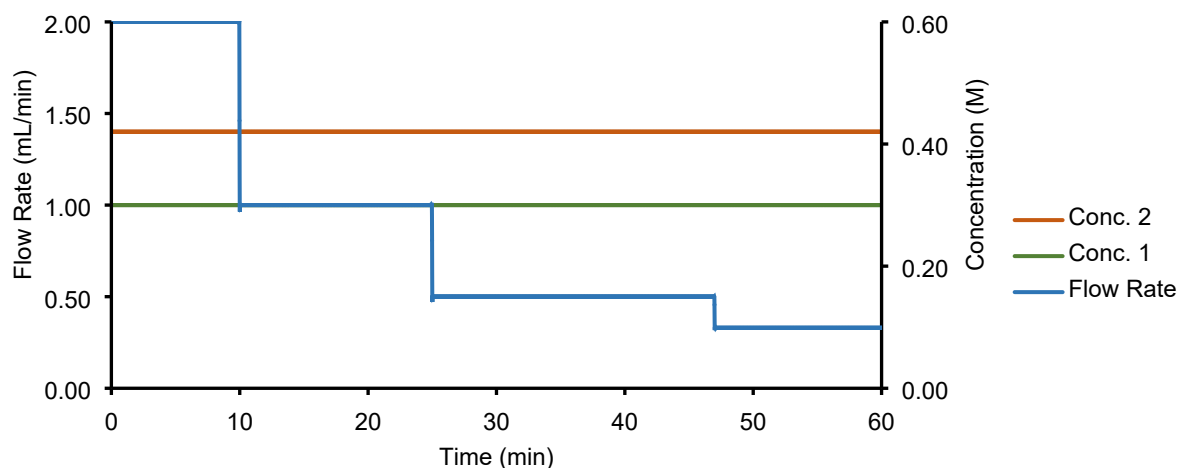


Figure S13. Experimental conditions for validation experiment at 75 °C using steady state conditions.

6.2 Comparison FTIR Data with UHPLC Data

Mass balance from FTIR and UHPLC data were compared to the input concentration of 2,5-hexandione (**2**). A mass balance was calculated as sum of 2,5-hexandione (**2**), product (**3**) and two times overreacted product (**4**) (**Figure S14**). UHPLC data were used for kinetic fitting as the mass balance from UHPLC data showed slightly better alignment with the input concentration of **2** than the FTIR data.

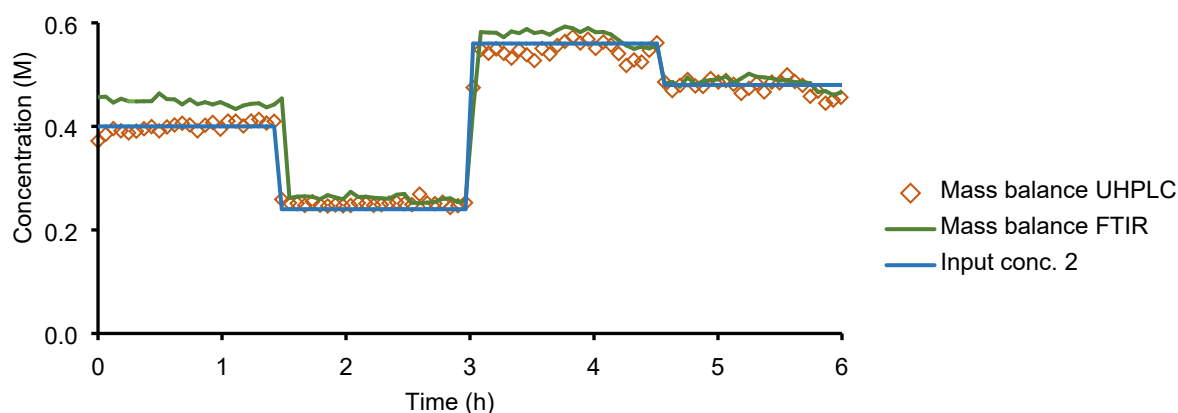


Figure S14. Comparison mass balance FTIR and UHPLC data with input concentration of 2,5-hexandione.

7 Kinetic Fitting of the Paal-Knorr Pyrrole Reaction in Dynochem

A kinetic model based on kinetic rate equations, neglecting axial dispersion was built in Dynochem (Scale-up Systems) using a simple batch model. Dynochem uses a modified Arrhenius equation (**Equation 6**), with k_{ref} at a reference temperature within the experimental range instead of an Arrhenius factor A.

$$k = k_{ref} \cdot e^{-\frac{E_a}{R} \cdot \left(\frac{1}{T} - \frac{1}{T_{ref}} \right)} \quad (6)$$

Two different models were defined using a reference temperature of 75°C. Initially the experiments at 75 °C were used to fit the k values and in a next step, experiments at different temperatures were included to fit all parameters simultaneously. Experiments 2, 3, 5, 7, 8, 10, 12, 13 and 14 (**Table S2**) were used for building the model, whereas experiments 1, 4, 6, 9, 11 (**Table S2**) and a steady state experiment (**Section 6.1**) were used for model validation. Alignment of the predicted data from the model with the experimental data is shown in **Figure S15** and **Figure S16** and in the parity plots (**Figure S17**).

Model 1:

Reaction 1: 2,5-hexandione + ethylenediamine → product + 2 water

Reaction 2: 2,5-hexandione + product → overreacted product + 2 water

Model 2:

Reaction 1: 2,5-hexandione + ethylenediamine → intermediate 1

Reaction 2: intermediate 1 → product + 2 water

Reaction 3: 2,5-hexandione + product → intermediate 2

Reaction 4: intermediate 2 → overreacted product + 2 water

Table S3: Summary of the kinetic parameters for each of the two models at a reference temperature of 75°C.

Model 1			Model 2		
k₁	0.0195 L/mol s	± 12 %	k₁	0.0195 L/mol s	± 12
E_{a,1}	4.67 kJ/mol	low sensitivity	E_{a,1}	4.67 kJ/mol	low sensitivity
			k₂	620 1/s	low sensitivity
			E_{a,2}	60.8 kJ/mol	low sensitivity
k₂	0.000354 L/mol s	± 5.9%	k₃	0.000354 L/mol s	± 5.9%
			k₄	267 1/s	low sensitivity
Selection criterion	3.347		3.347		

Only small amounts of overreacted product (**4**) were formed and this reaction is only slightly temperature-dependent under the conditions studied. Therefore, the activation energy was fixed at 0 kJ/mol for this step. Formation of product (**3**) shows a low temperature dependence as well and the fitting resulted in low sensitivity of E_{a,1}. Increasing complexity (Model 2) does not improve the kinetic fitting as Model 1 and Model 2 resulted in the same selection criterion and same values for the parameters.

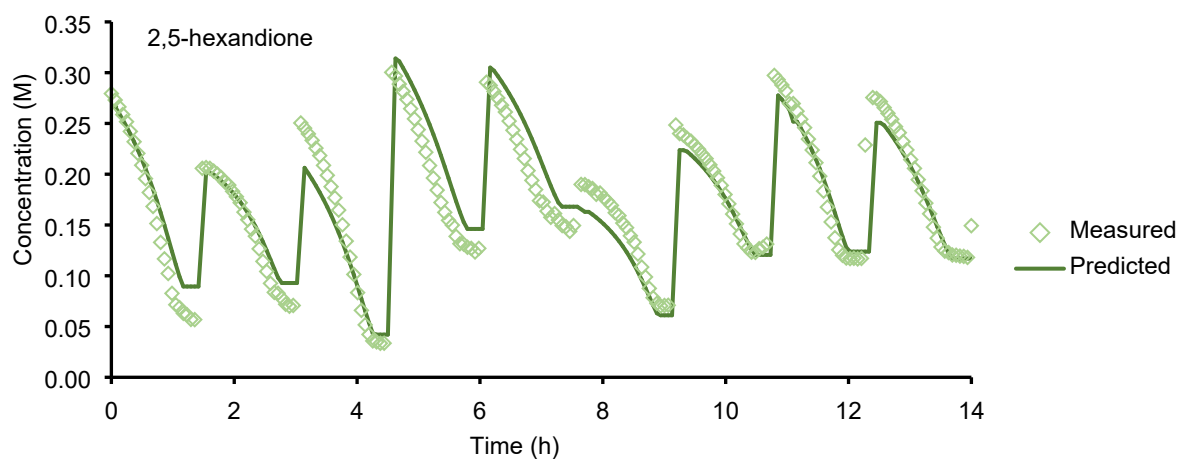


Figure S15. Measured and model predicted concentration of 2,5-hexandione (**2**) for experiments 2, 3, 5, 7, 8, 10, 12, 13 and 14.

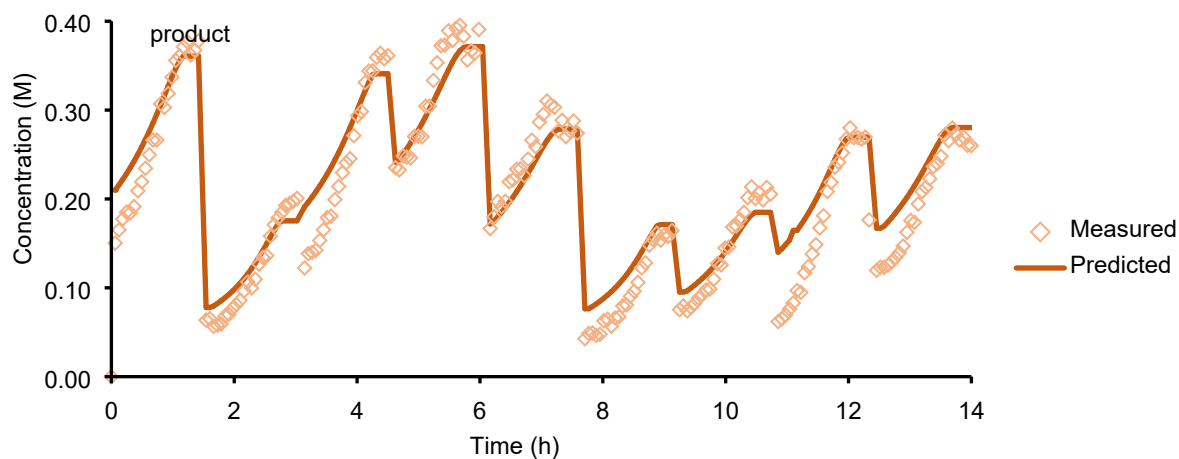


Figure S16. Measured and model predicted concentration of product (**3**) for experiments 2, 3, 5, 7, 8, 10, 12, 13 and 14.

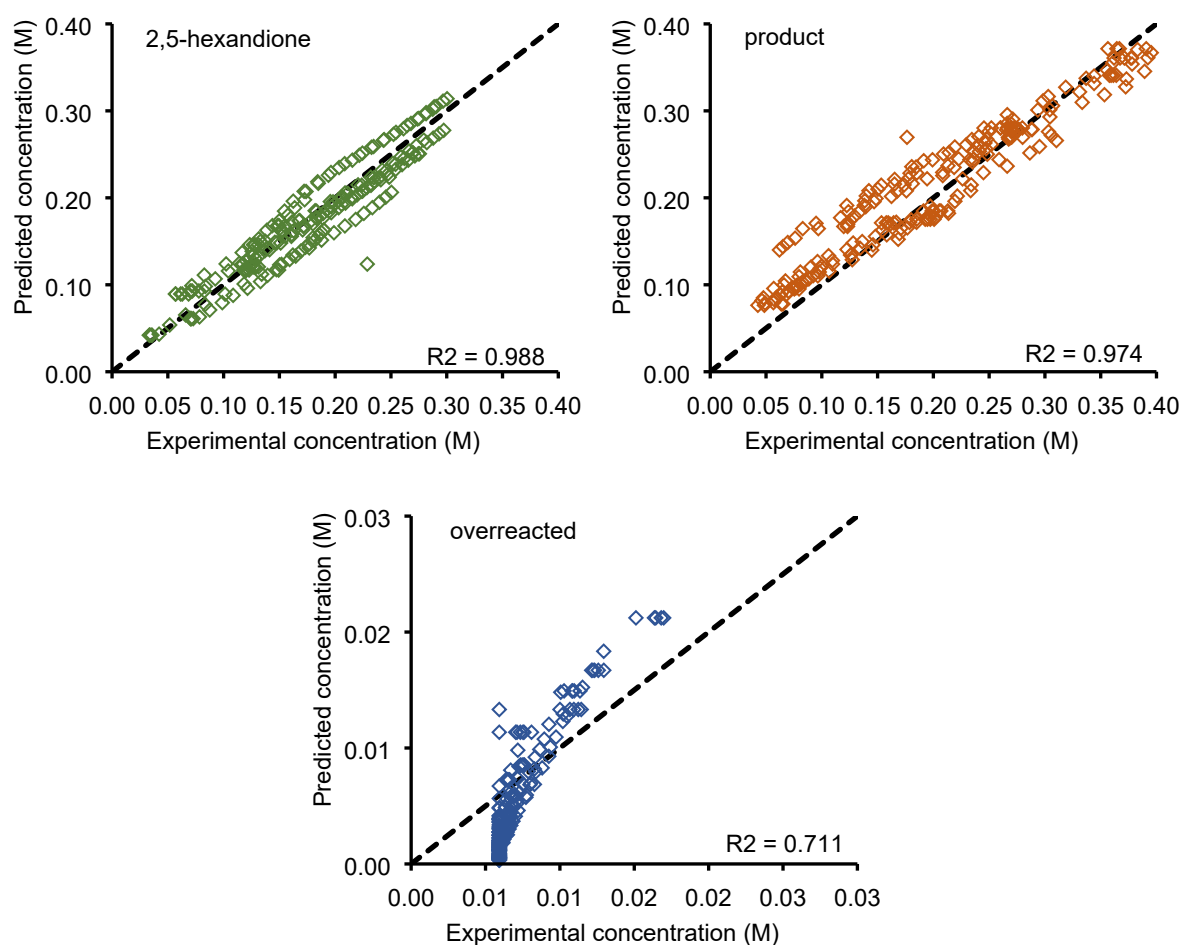


Figure S17. Parity plots for reaction components 2,5-hexandione (**2**) (top left), product (**3**) (top right) and overreacted product (**4**) (bottom middle) for experiments 2, 3, 5, 7, 8, 10, 12, 13 and 14.

7.1 Model Validation

Experiments 1, 4, 6, 9 and 11 from **Table S2** and a steady state experiment (**Section 6.1**) were used for model validation. Parity plots for the alignment between the measured and the predicted concentration are shown in **Figure S18** and **Figure S19**.

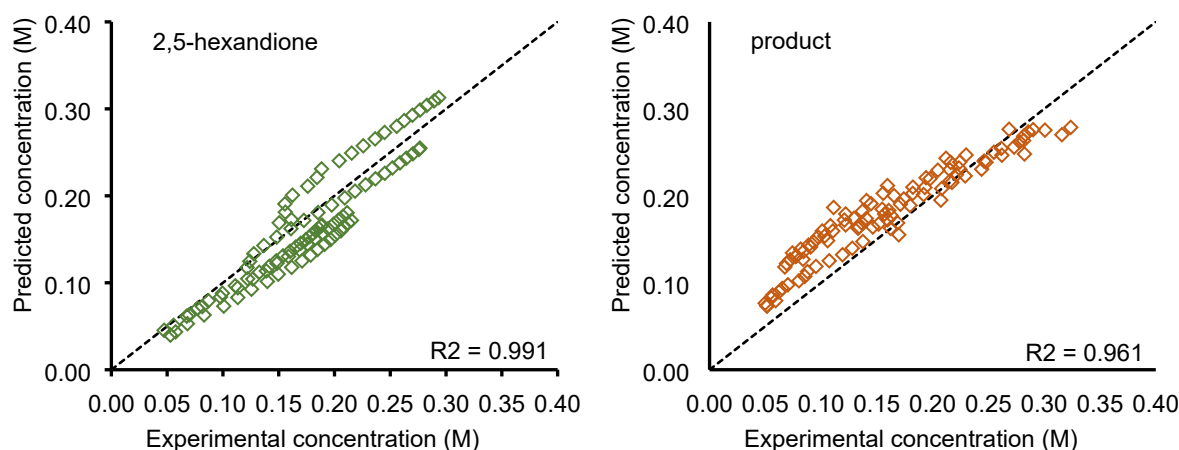


Figure S18. Parity plots for reaction components 2,5-hexandione (**2**) (left) and product (**3**) (right) for experiments 1, 4, 6, 9, 11 from Table S2.

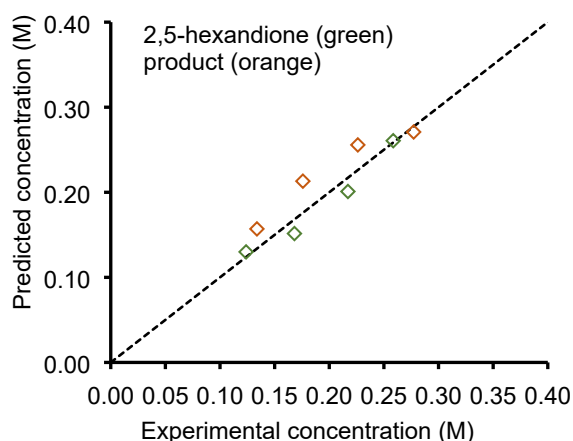


Figure S19. Parity plot for reaction components 2,5-hexandione (**2**) and product (**3**) for steady state validation experiment described in Section 6.1.

8 Dynamic Experiments: Telescoped Reaction

The process setup is shown in **Figure S3** and described in **Section 2**. The Paal-Knorr pyrrole reaction was operated at constant conditions with a flow rate of 0.3 mL/min for each pump. This was started 1 h earlier than the S_NAr reaction to accumulate sufficient material in the reservoir. 2,5-hexandione (**2**) was used in 1.2 equiv. to ensure full conversion of ethylenediamine. Dynamic experiments for the S_NAr reaction were performed at constant temperature and constant concentration of starting materials while linearly varying the flow rate. Experiments started at 1 mL/min. After 15 min the flow rate was linearly decreased from 1 mL/min to 0.33 mL/min within 30 min, followed by steady state conditions at 0.33 mL/min for 22 min. Equivalents of product (**3**) in relation to 2-fluornitrobenzene (**5**) (**Table S4**) are based on full conversion of ethylenediamine (**1**) to product (**3**) in the Paal-Knorr reaction. The actual concentration in the reaction stream was calculated according to the inline FTIR measurements at the reactor inlet. This allowed correction of minimal concentration changes within experiments.

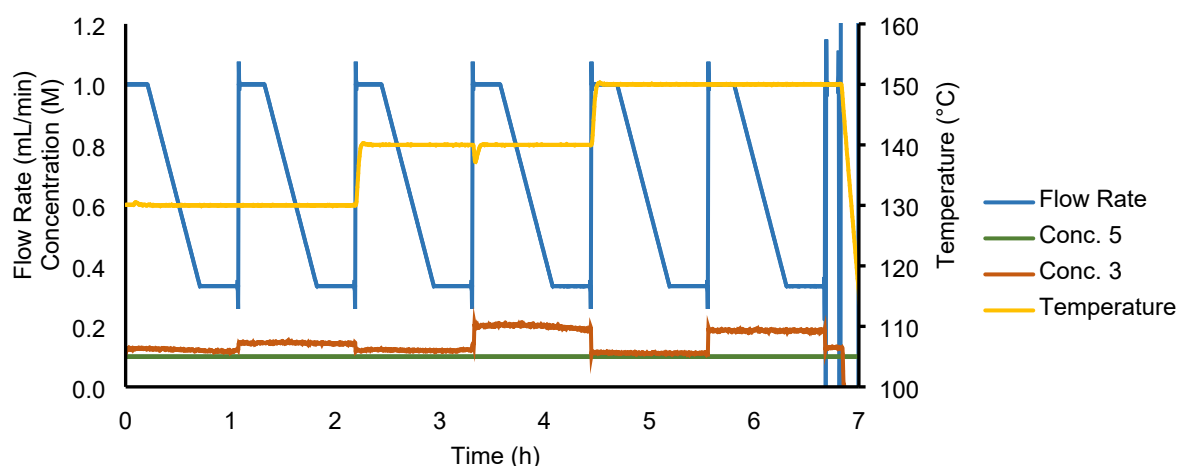


Figure S20: Experimental conditions for experiments 1-6. Linear variation of flow rate at temperatures from 130-150°C while concentration of 2-fluoronitrobenzene (**5**) and product (**3**) (FTIR measurement) remain constant for each experiment.

Table S4: Conditions for dynamic experiments of the S_NAr reaction. Molar concentration 2-fluoronitrobenzene (**5**), equivalents product (**3**) and reactor temperature.

Exp	Conc. 2-fluoronitrobenzene (M)	Equiv. product (3)	T (°C)
1	0.1	1.2	130
2	0.1	1.4	130
3	0.1	1.2	140
4	0.1	2.0	140
5	0.1	1.2	150
6	0.1	2.0	150

8.1 Validation Experiments

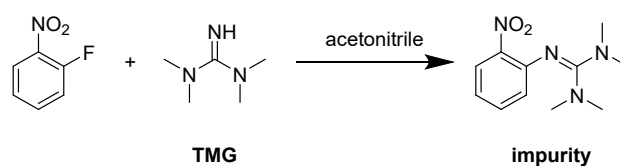
Validation experiments using higher equivalents of product (**3**) were performed using the same dynamic experimental design (**Table S5**). Stock solutions for the Paal-Knorr reaction were used in concentrations of 1.60 M for ethylenediamine and 1.92 M for 2,5-hexandione.

Table S5: Experimental conditions for validation experiments. Molar concentration 2-fluoronitrobenzene (**5**), equivalents product (**3**) and reactor temperature.

Exp	Conc 2-fluoronitrobenzene (M)	Equiv. product (3)	T (°C)
1	0.1	4.0	140
2	0.1	6.0	140

8.2 Mass Balance

In the S_NAr reaction an impurity (**8**) was formed from 2-fluornitrobenzene (**5**) and TMG (**6**) (**Scheme S1**), that can be assigned to peak **a** in the chromatogram (**Figure S7**) and identified by its mass from LC-MS. Therefore, an error in the mass balance from 2-fluoronitrobenzene (**5**) and S_NAr product (**6**) was observed. This error was significantly reduced by using 2-*tert*-butyl-1,1,3,3-tetramethylguanidine (^{*t*}BuTMG) instead of TMG as base (**Figure S21**).



Scheme S1. Impurity formation.

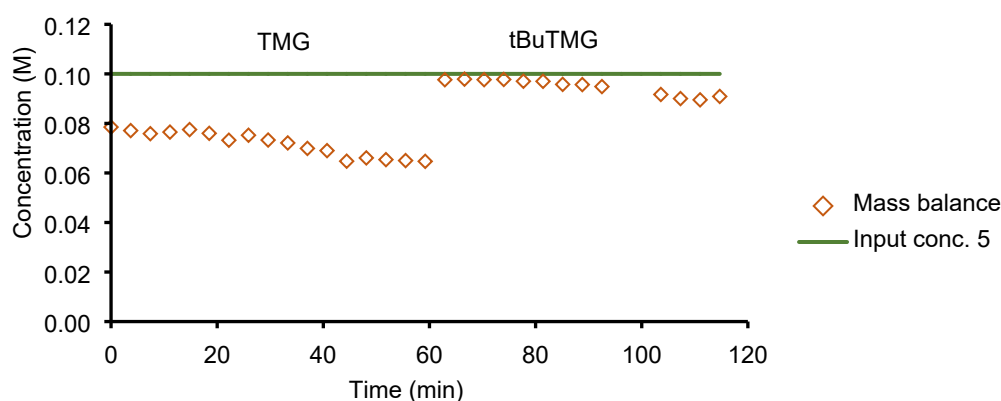


Figure S21. Comparison mass balance of S_NAr experiments using TMG or $tBuTMG$ as base. Impurity formation is not possible with $tBuTMG$. Dynamic experiments at 140 °C using 2.0 equiv. product (3).

9 Kinetic Fitting of the Nucleophilic Aromatic Substitution in Dynochem

A kinetic model including S_NAr product (7) formation, impurity (8) formation and HF capture, was fitted using Dynochem (**Figure S22**, **Figure S23**, **Figure S24**). The concentration of 8 was calculated as residual of the mass balance to the input concentration of 2-fluoronitrobenzene (5).

Model:

Reaction 1: 2-fluoronitrobenzene + product $\rightarrow S_NAr$ product + HF

Reaction 2: 2-fluoronitrobenzene + TMG \rightarrow impurity + HF

Reaction 3: HF + TMG \rightarrow TMG \cdot HF

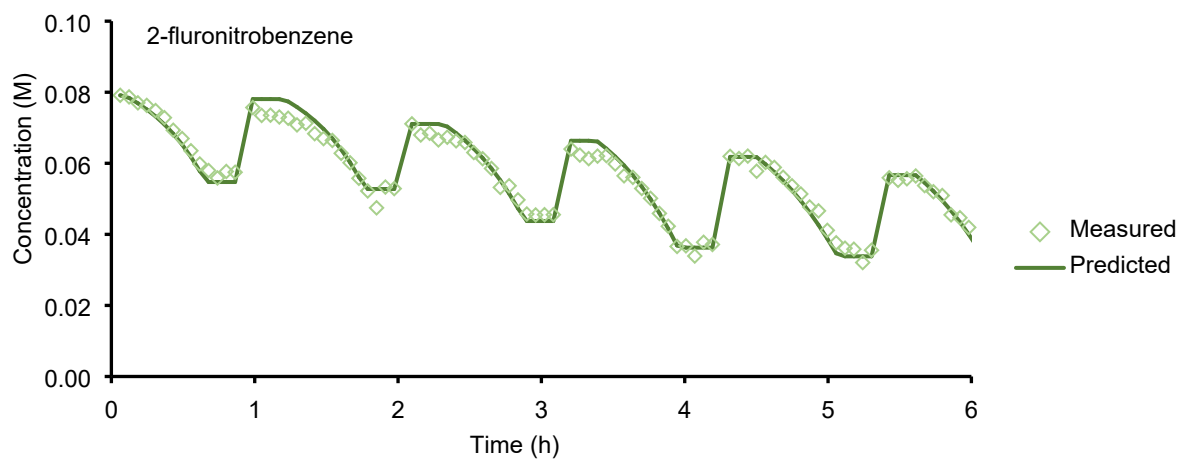
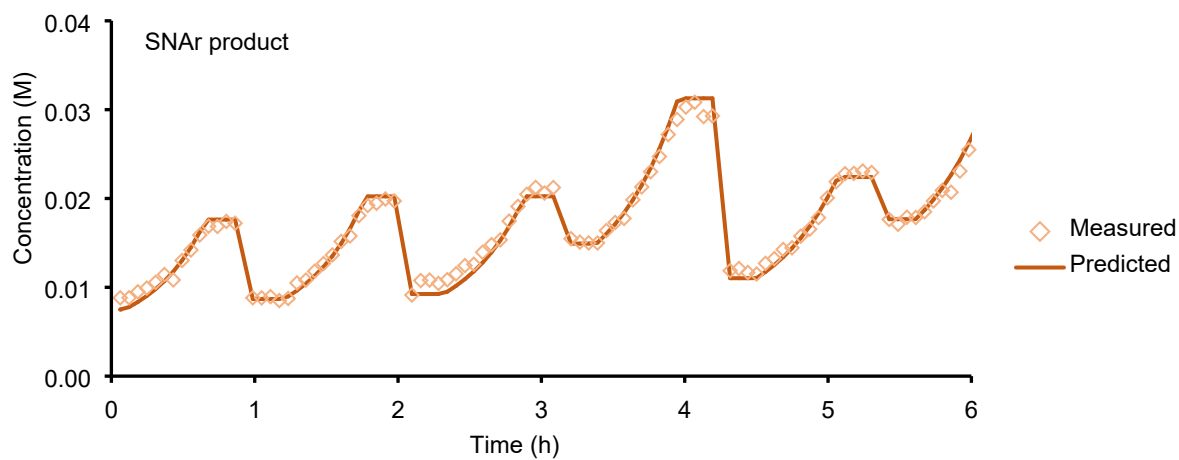
Reaction 3 was assumed to be very fast and therefore the parameters were fixed to 100 L/mol s for k_{ref} and 0 kJ/mol for E_a . The reference temperature was set to 140 °C.

Table S6: Kinetic parameters for the S_NAr reaction at a reference temperature of 140 °C.

k_1	0.00513 L/mol s	$\pm 1.5 \%$
$E_{a,1}$	40.8 kJ/mol	$\pm 6.2 \%$
k_2	0.00894 L/mol s	$\pm 1.8 \%$
$E_{a,2}$	72.6 kJ/mol	$\pm 4.4 \%$
k_3	100 L/mol s	fixed
$E_{a,3}$	0 kJ/mol	fixed

Table S7: Correlation Matrix for the kinetic parameters of the S_NAr reaction

	k_1	k_2	$E_{a,1}$	$E_{a,2}$
k_1	1	0.351	0.151	0.133
k_2	0.351	1	0.132	0.207
$E_{a,1}$	0.151	0.132	1	0.344
$E_{a,2}$	0.133	0.207	0.344	1

**Figure S22.** Measured and model predicted concentration of 2-fluoronitrobenzene (**5**) for experiments 1-6.**Figure S23.** Measured and model predicted concentration of S_NAr product (**7**) for experiments 1-6.

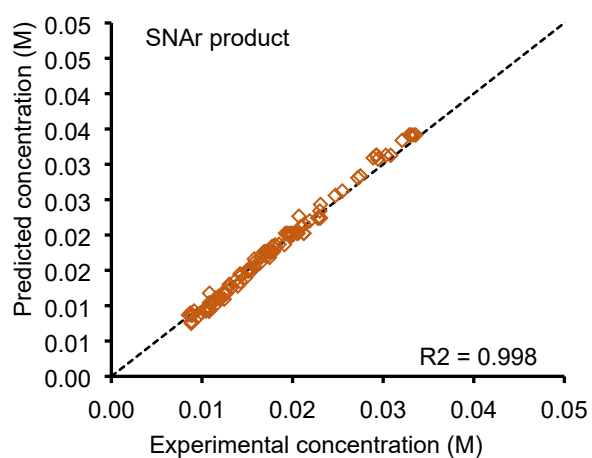
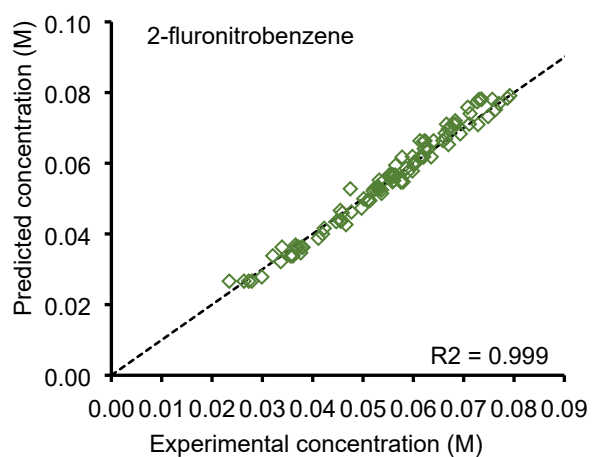


Figure S24: Parity plots 2-fluoronitrobenzene (**5**) (left) and S_NAr product (**7**) (right).

9.1 Validation Kinetic Model

The developed kinetic model was validated by simulating the experiments listed in **Table S2** and show good alignment with the model (**Figure S25**).

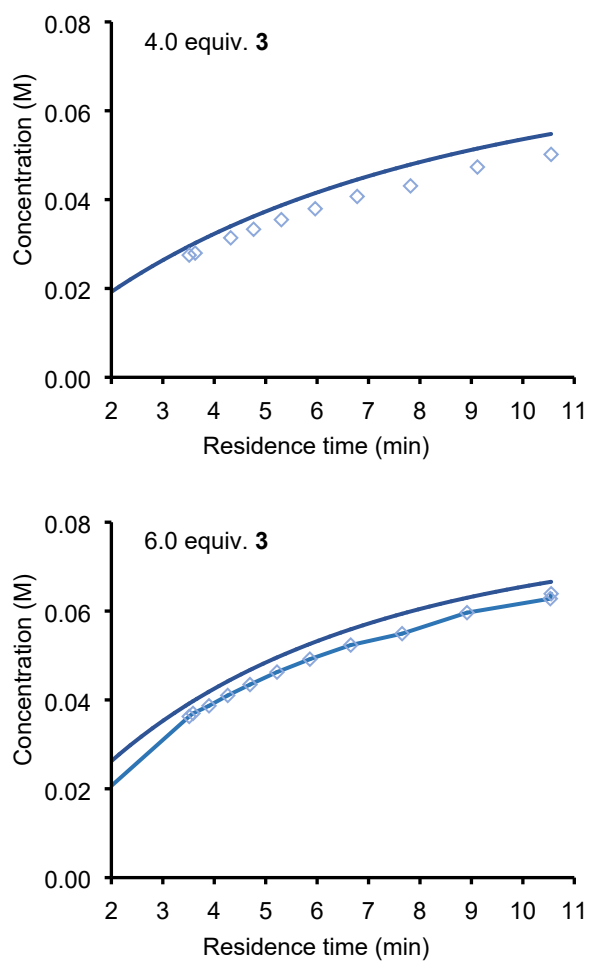


Figure S25. Results model validation. Comparison predicted concentration (line) with measured concentration (dots) of S_NAr product (7) for the validation experiments using 4.0 equiv. and 6.0 equiv. **3** at 140 °C.

10 References

- [1] O. Levenspiel, *Chemical Reaction Engineering*, **1999**.
- [2] C. Waldron, A. Pankajakshan, M. Quaglio, E. Cao, F. Galvanin, A. Gavrilidis, *React. Chem. Eng.* **2020**, 5, 112–123.